THE JOURNAL OF PHYSICAL CHEMISTRY Letters

Letter

pubs.acs.org/JPCL

Emergence of Hysteresis and Transient Ferroelectric Response in Organo-Lead Halide Perovskite Solar Cells

Hsin-Wei Chen,[†] Nobuya Sakai,[‡] Masashi Ikegami,[†] and Tsutomu Miyasaka*,[†]

[†]Graduate School of Engineering, Toin University of Yokohama, 1614 Kuroganecho, Aoba, Yokohama 225-8503, Japan

[‡]Clarendon Laboratory, University of Oxford, Parks Road, Oxford OX1 3PU, United Kingdom

Supporting Information

ABSTRACT: Although there has been rapid progress in the efficiency of perovskite-based solar cells, hysteresis in the current–voltage performance is not yet completely understood. Owing to its complex structure, it is not easy to attribute the hysteretic behavior to any one of different components, such as the bulk of the perovskite or different heterojunction interfaces. Among organo-lead halide perovskites, methylammonium lead iodide perovskite ($CH_3NH_3PbI_3$) is known to have a ferroelectric property. The present investigation reveals a strong correlation between transient ferroelectric polarization of $CH_3NH_3PbI_3$ induced by an external bias in the dark and hysteresis enhancement in photovoltaic characteristics. Our results demonstrate that the reverse bias poling (−0.3 to −1.1 V) of $CH_3NH_3PbI_3$ photovoltaic layers prior to the photocurrent–voltage measurement generates stronger hysteresis whose extent changes significantly by the cell architecture. The phenomenon is interpreted as the effect of remanent polarization in the perovskite film on the photocurrent, which is most enhanced in planar perovskite structures without mesoporous scaffolds.

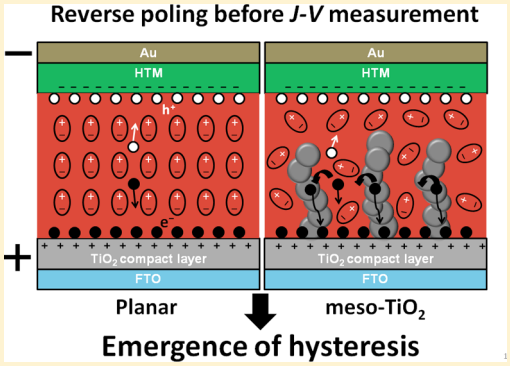

Rapid progress in conversion efficiency of organic-lead halide perovskite solar cells has attracted worldwide researchers to make a lot of effort to develop methods to create solution-processable hybrid crystals as absorber materials.[1−7] The hybrid perovskites solar cells have demonstrated high solar energy conversion efficiencies for both planar structures[7] and mesoporous structures using Al_2O_3,[3] TiO_2,[6] and ZrO_2[8] scaffolds. However, hysteretic behavior in power generation that accompanies the current–voltage performance of the perovskite has emerged as a critical issue to be tackled for reliability and stability. It is still unclear which structure of perovskite cells performs better or is beneficial over others without hysteresis.[9] The contact interfaces and defects surrounding the perovskite are assumed to have a big effect on the extent of hysteresis. This possibility is considered by the fact that little or no hysteresis occurs for specific structures such as inverted planar structured perovskite cells.[10] Besides, intrinsic polarization of the organic-lead halide perovskite as a ferroelectric material is also an important factor influencing the hysteresis.[11−13] Hysteresis phenomena during photocurrent density–voltage (J–V) measurements have been observed in both mesoporous and planar structures, and the latter generally exhibits large hysteresis. Some groups proposed that slow transients and photoconductivity difference of the perovskite give rise to hysteresis in J–V measurements at different scan rates and directions.[11−17] Here, the intrinsic ferroelectric property of the perovskite can severely affect the J–V measurement that determines the cell efficiency. It has been established that methylammonium lead iodide perovskite ($CH_3NH_3PbI_3$), widely used as a high-efficiency photovoltaic semiconductor, has the ferroelectric property.[12] Although this semiconductor is considered to exhibit a weak ferroelectricity in the form of a bulk crystal, ferroelectric behavior can be enhanced when it is in the form of a thin film surrounded by a metal oxide conductor and insulator materials. It has been clarified by impedance measurements that $CH_3NH_3PbI_3$ photovoltaic films exhibit a giant dielectric constant and its polarization is amplified by external voltage and illumination, in which an additional capacitance at low frequency caused by slow dynamic processes in the cells gives rise to hysteresis in J–V measurements.[18,19] Wei et al. have analyzed the ferroelectric behavior of $CH_3NH_3PbI_{3-x}Cl_x$ films in relation to the dielectric constant as a function of polarization under a scanning voltage.[12] In this Letter, we show a strong correlation between J–V hysteresis of photovoltaic cells and ferroelectric polarization of $CH_3NH_3PbI_3$ induced by reverse bias poling for different cell architectures.

Perovskite solar cells with different structures were fabricated under ambient air conditions, and the details are described in the Supporting Information (SI). Three structures that give large differences in the magnitude of hysteresis were investigated. They were mesoporous structures using scaffolds of TiO_2 and Al_2O_3 and a planar structure without scaffolds. The cell structure using mesoporous scaffold is FTO-glass/compact

Received: November 17, 2014
Accepted: December 15, 2014
Published: December 15, 2014

Scheme 1. Schematic Illustration of the Organo-Lead Halide Perovskite Solar Cells in Planar Structures, Mesoporous TiO_2, and Al_2O_3 Scaffolds under Applied Electric Field, and Physical Mechanism of the Polarization in Ferroelectric Perovskite

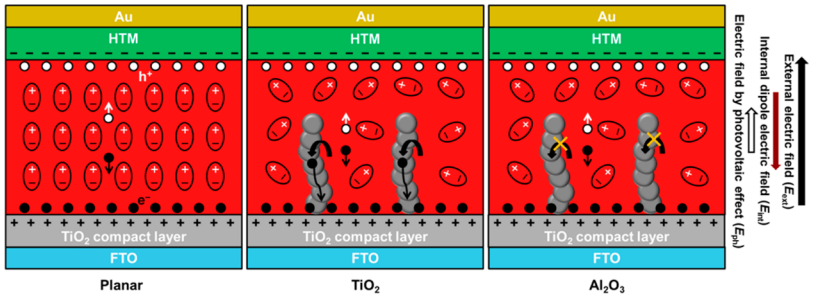

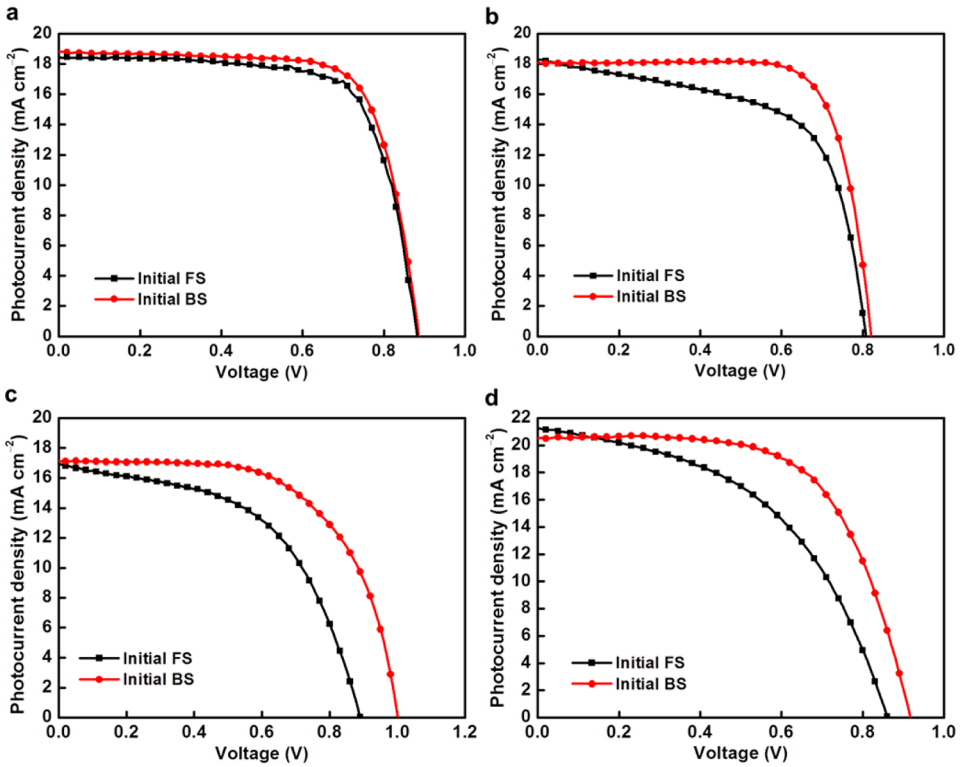

Figure 1. *J*–*V* curves with initial FS and BS of *meso*-TiO_2 (a) without and (b) with hysteresis, (c) *meso*-Al_2O_3, and (d) planar-structure-based perovskite solar cells under 1 sun illumination.

TiO_2 (~50 nm)/mesopopous TiO_2 or Al_2O_3 (~300 nm)/$CH_3NH_3PbI_3$ (~300 nm)/hole transport materials (HTMs; here, spiro-MeOTAD)/Au (~100 nm), as shown in Figure S1 (SI). Here, cell structure can be characterized as a p–i–n junction employing $CH_3NH_3PbI_3$ as an intrinsic semiconductor with a band gap of 1.55–1.60 eV. However, unlike traditional p–i–n junction solar cells, $CH_3NH_3PbI_3$ has a large dielectric constant on the order of 10^1–10^3 depending on the frequency range of 10^{-1}–10^3 Hz.[19] The dielectric constant is further enhanced by external-bias polarization[11,18,20] and illumination.[19] When photocurrent is generated in ferroelectric perovskite, the built-in electric field formed by photocurrent (E_{ph}) is exposed to internal polarization (E_{int}) due to dipoles, which is enhanced by the external-bias electric field (E_{ext}), that is, the applied voltage. Scheme 1 depicts the situation of E_{ext} and E_{int}. Here, the negative (reverse) poling of Au, that is, the applied negative voltage at Au, gives an E_{ext} in the direction from FTO to Au. Taking an example of a perovskite layer ~300 nm in thickness, a bias voltage of −0.9 V corresponds to E_{ext} as large as -3×10^6 V m^{-1}. This large E_{ext} develops a ferroelectric polarization inside of the perovskite layer and internally causes an electric field, E_{int}, in the direction against E_{ext}, as shown in Scheme 1. Ferroelectricity of perovskite allows E_{int} to remain as a remanent (nonrelaxed) polarization in the layer unless opposite (positive) poling is further applied. On the basis of this relationship, the focus of our study was to show how the remenant E_{int} influences the *J*–*V* characteristics of the perovskite photovoltaic cell.

Photovoltaic performance of the perovskite cells were found to be strongly influenced by structural differences. Figure 1 shows the hysteretic behavior in *J*–*V* characteristics, measured under 1 sun illumination, for four different structures, two mesoporous TiO_2 (*meso*-TiO_2) scaffolds, a mesoporous Al_2O_3 (*meso*-Al_2O_3) scaffold, and a planar structure without mesoporous scaffolds. Here, we had two kinds of *meso*-TiO_2 structures, which had essentially the same thickness and morphology of the TiO_2 mesoporous layer but differed in the morphology of the perovskite; one had a large volume of the capping layer on the surface of TiO_2, while the other had much less capping layer. The *meso*-TiO_2 cell with a larger volume of

dx.doi.org/10.1021/jz502429u | J. Phys. Chem. Lett. 2015, 6, 164–169

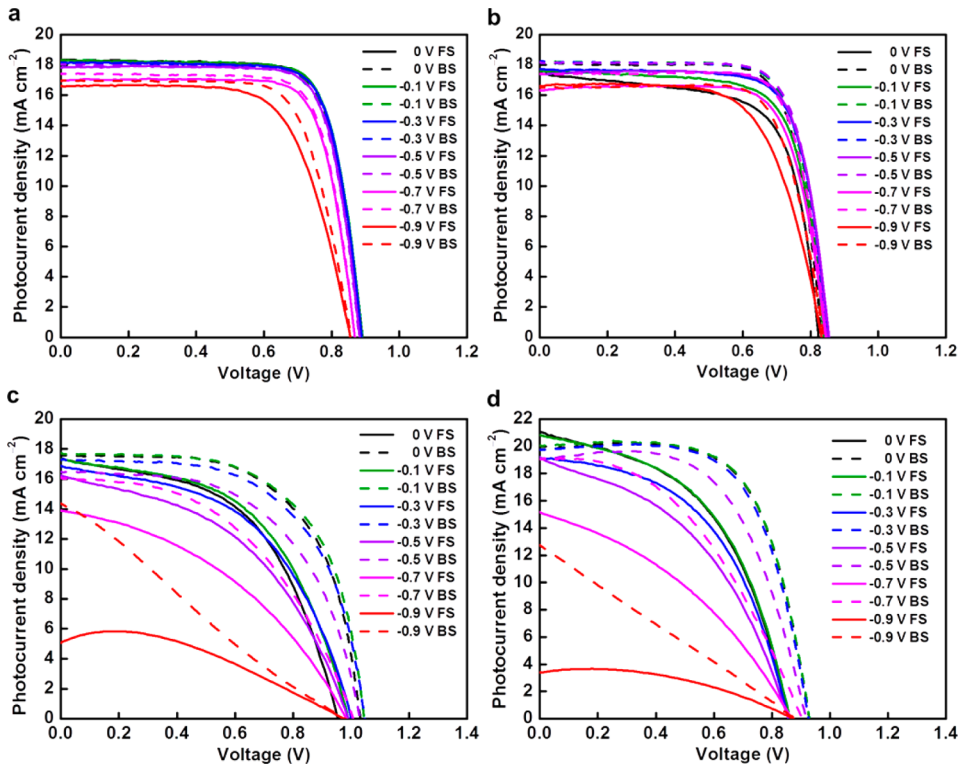

Figure 2. $J-V$ curves with FS and BS of mesoporous TiO_2 (a) without and (b) with hysteresis, (c) Al_2O_3, and (d) planar-structure-based perovskite solar cells under 1 sun illumination. All cells were applied at various bias voltages in the dark for 5 min before the $J-V$ measurements.

capping layer was found to exhibit hysteresis with larger photocurrent density for backward scan (BS) than that for forward scan (FS), accompanied by larger V_{OC} in the BS. In contrast, the other *meso*-TiO_2 with a poorly covered capping layer showed lesser hysteresis with a slight change in V_{OC}. As the thickness of the perovskite capping layer decreases, hysteresis behavior becomes weaker. However, hysteresis in the case of *meso*-Al_2O_3 and planar structures was found to be significant, resulting in a large difference in the open-circuit voltage (V_{OC}) measured during BS and FS. This indicates that the $J-V$ hysteresis behavior gradually disappears when the architecture evolves from a planar heterojunction type to a *meso*-TiO_2 scaffold type by confining more perovskite crystals into the mesopores.[12]

Polarization of $CH_3NH_3PbI_3$ and its effect on the $J-V$ characteristics was investigated by exposing the cell to an external electric field without illumination (i.e., poling) that causes internal polarization, as shown in Scheme 1. The perovskite cells of different structures showing hysteresis to different extents were subjected to external bias poling prior to the $J-V$ measurement. The conditions of external bias are known to have a big effect on the device performance, as studied by Unger et al.[17] Here, we conducted a reverse bias poling of the cell, which corresponds to the a condition where the cell is biased with a negative voltage before the start (zero voltage) of illumination and $J-V$ measurement. The cells of four different structures (two mesoporous TiO_2 scaffolds with small and large hysteresis, an Al_2O_3 scaffold, and a planar structure) were poled in the open-circuit condition at various negative voltages up to −0.9 V in the dark for 5 min. $J-V$ measurement under 1 sun illumination followed this poling. All of the measurements were taken on cells without encapsulation in an ambient atmosphere and at room temperature. We found that this poling had a substantial effect on hysteresis and cell performance. Figure 2 shows the results as the effect of reverse poling voltage on the FS and BS $J-V$ curves. Corresponding dark current curves of FS and BS are given in Figure S2 (SI). First, all results show as a general phenomenon that reverse (negative) poling of the cell before the $J-V$ scan decreases the photocurrent magnitude. This phenomenon occurs more clearly in the direction of FS, which gives lower current density than BS. Second, such suppression of photocurrent becomes more intense for the cell of more hysteric behavior. Especially strong influence is seen for *meso*-Al_2O_3 and planar structures that originally had large hysteresis as in Figure 1. Here, it is noteworthy that the photocurrent reduction in *meso*-Al_2O_3 and planar structures starts even with weak poling by −0.1 V, while such reduction is small for *meso*-TiO_2 structures. For a nonhysteretic type *meso*-TiO_2 structure, however, photocurrent reduction occurs for poling with a voltage more negative than −0.5 V.

It has been studied that organo-lead halide perovskites undergo a slow polarization due to a ferroelectric property, which is sensitive to applied bias.[11−16,20−22] As shown in Scheme 1, the external electric field, E_{ext}, introduced by reverse poling generates an array of dipoles, which gives an internal electric field, E_{int}, opposite to the direction of E_{ext}. When ferroelectricity of the thin film perovskite is sufficiently large, this E_{int} can remain to some extent unless positive poling is applied to offset the field. Upon generation of photocurrent, the direction of the electrons flow (from Au/HTM to FTO) becomes against the direction of remanent E_{int}. The remanent polarization is thus assumed to suppress the flow of photocurrent. This effect must be more enhanced for the perovskite layer structure that develops larger E_{int}, in other words, an ordered array of dipoles. Here, an ordered dipole

dx.doi.org/10.1021/jz502429u | J. Phys. Chem. Lett. 2015, 6, 164−169

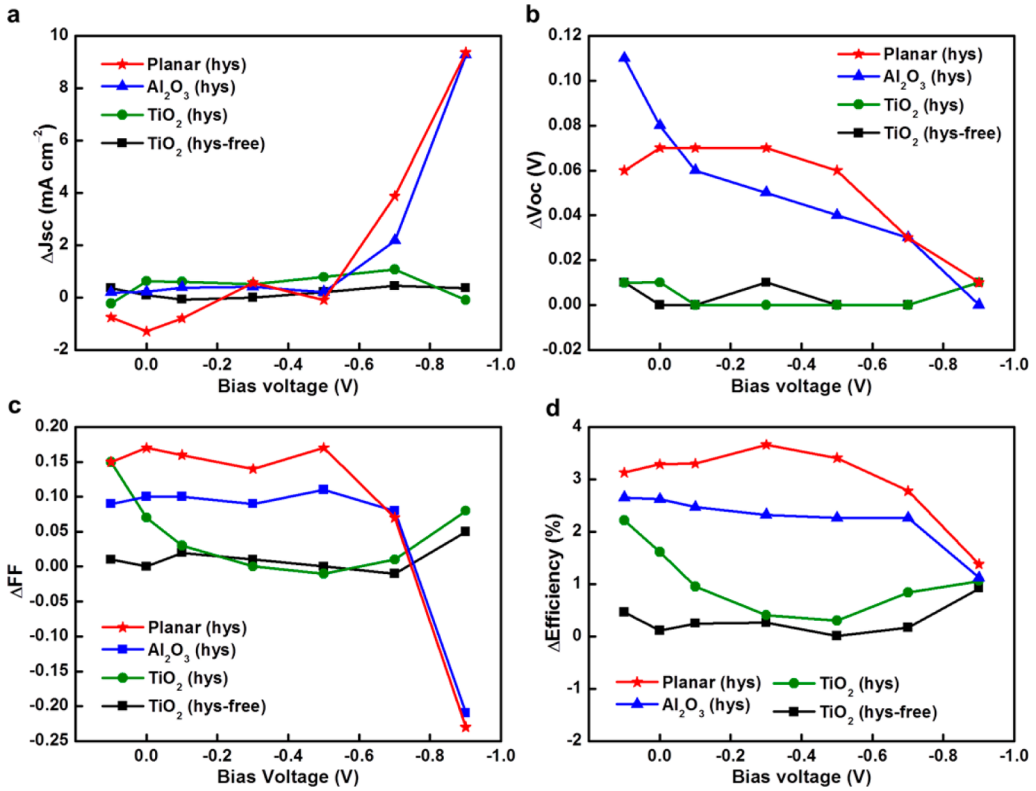

Figure 3. Difference (Δ) between FS and BS of *meso*-TiO_2 with and without hysteresis, Al_2O_3, and planar-structure-based perovskite solar cells in (a) J_{SC}, (b) V_{OC}, (c) FF, and (d) efficiency.

array can develop in a flat continuous (planar) structure of perovskite, while a more random orientation of dipoles can occur in mesoporous structures where ferroelectric domains of perovskites are weakened by reduced crystal size confined in mesopores. Planar and *meso*-Al_2O_3 structures have a common point in the carrier transfer process that the photocurrent flows all the way through the perovskite phase in the absence of an electron acceptor (TiO_2). Both structures thus have a strong effect of the dipole on the photocurrent flow. This is not the case in *meso*-TiO_2, where photogenerated electrons in the perovskite domains are captured by TiO_2 surface before their movement is controlled by dipoles. Hysteresis can thus be suppressed when most of perovskites are confined in the mesoporous interior with little capping layer. However, for the *meso*-TiO_2 sample which had a large capping layer of perovskite, hysteresis appears as a result of remanent polarization in the capping layer. The morphology of the hysteretic *meso*-TiO_2 structure (with a capping layer) and the strongly hysteretic planar structure observed by a scanning electron microscope (SEM) are shown in Figure S1 (SI). On the basis of the effect of polarization, the FS course in the $J-V$ scan gives lower current density than the BS course because photocurrent is restricted by remanent reverse polarization at the start of FS (zero voltage) while the polarization is relaxed by forward bias at the start of BS (V_{OC}). Here, the dielectric constant is considered to become large at V_{OC} where ferroelectric restraint of dipoles is minimized and an increased dielectric constant leads to enhanced photocurrent.[12] We observed that hysteresis tends to be more enhanced by an increased rate of scan. In FS, the voltage scan from zero to V_{OC} will cause rearrangement of dipoles. When the scan rate is higher, dipole rearrangement cannot follow the voltage change and hysteresis increases. Slow response of the dipole change on the order of seconds that explains the large scan rate dependence has been reported for $CH_3NH_3PbI_{3-x}Cl_x$.[12,15] The fact that such a poling effect on the $J-V$ scan is observed at a low poling voltage of −0.1 V for planar structures implies that internal polarization of perovskite, E_{int}, can be very sensitive to the bias condition prior to the $J-V$ measurement. In addition to reverse poling treatment, we found that forward bias poling of the cells in the dark was found to diminish the extent of hysteresis. This may be reasonable when taking into account that E_{int} generated by forward poling has the same direction as the photocurrent. A similar result has been reported by Snaith group.[16] Our discovery in this study corroborates that the cell structure accommodating the perovskite has a strong effect in the polarization of the perovskite prior to the $J-V$ measurement and changes the extent of hysteresis.

The differences of the photovoltaic parameter (J_{sc}, V_{OC}, FF, and efficiency) between FS and BS in $J-V$ characteristics are plotted against the applied poling voltage, and the results for the four cell structures are summarized in Figure 3, where the change (Δ) represents the value at BS minus the value at FS. We can clearly see that the *meso*-Al_2O_3 structure has a similar behavior to the planar structure in the hysteresis enhancement by poling treatment. Hysteresis behavior also changes when scanned at different starting points; the efficiency decreases significantly when the scan starts from a more negative bias voltage. Different starting points would lead to different initial states of the ferroelectric domain.[12,13] In Figure 3, a large effect in increasing hysteresis is occurring at a voltage more negative than −0.5 V. Although J_{SC} tends to be stable under poling at a small negative voltage, a large increase in ΔJ_{SC} in BS takes place beyond this threshold voltage, accompanied by drops in ΔFF

dx.doi.org/10.1021/jz502429u | J. Phys. Chem. Lett. 2015, 6, 164−169

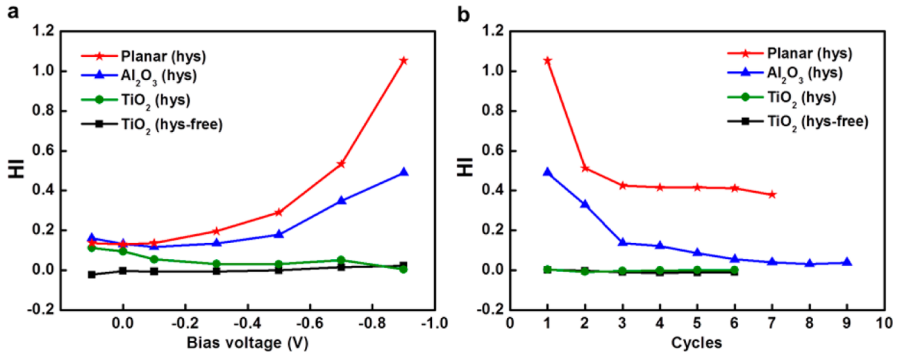

Figure 4. (a) HI for perovskite solar cells of nonhysteretic and hysteretic *meso*-TiO_2, *meso*-Al_2O_3, and planar structures as a function of poling bias voltage. HI is derived from $J-V$ curves of cells that underwent reverse bias poling as in Figure 2. (b) Change of HI by a repeated cycle of the $J-V$ curve scan. The cells were poled at −0.9 V.

and ΔV_{OC}. In contrast, two *meso*-TiO_2 structures undergo relatively smaller change although hysteresis still persists. For more quantitative comparison of the hysteresis between different cell structures, the dimensional hysteric index (HI) was derived from the results shown in Figure 2. HI is defined as[15]

$$\mathrm{HI} = \frac{\left(J_{BS}\left(\frac{V_{OC}}{2}\right) - J_{FS}\left(\frac{V_{OC}}{2}\right)\right)}{J_{BS}\left(\frac{V_{OC}}{2}\right)} \quad (1)$$

Here, $J_{BS}(V_{OC}/2)$ is the photocurrent at half V_{OC} for the BS, while $J_{BS}(V_{OC}/2)$ is the photocurrent at half V_{OC} for the FS. A HI of 0 corresponds to a cell without hysteresis, while a HI of 1 represents the case where the hysteresis is as high as the magnitude of the photocurrent. The results of the HI as well as photovoltaic parameters for *meso*-TiO_2, Al_2O_3, and planar structures are listed in Tables S1−S4 (SI), respectively. In Figure 4, HI values of different structures are plotted against the bias voltage and also investigated as a function of the number of scan cycles between 0 V and V_{OC}. These plots clearly show the influence of the structural difference on the hysteresis. HI values of *meso*-TiO_2 structures stay around 0 with minimal hysteresis. In contrast, planar and *meso*-Al_2O_3 show large HI with an increase in bias voltage (Figure 4a). Here, an important behavior is found in the cyclic measurement (Figure 4b). Repeated $J-V$ scanning of the illuminated planar and *meso*-Al_2O_3 cells that had been poled at −0.9 V exhibited an effect of mitigation of the hysteretic behavior. The continuous change in $J-V$ curves during the scan cycle for the four different structures is shown in Figure S3 (SI). We also found that these changes in $J-V$ hysteresis were reversible. From the aspect of ferroelectric polarization, recovery of a less hysteretic property by cyclic scan can be interpreted as relaxation of dipoles from a highly ordered state (under reverse bias) to more random state by exposure of a cell to forward (positive) bias. This phenomenon agrees well with the fact that forward bias poling of the hysteretic cells before $J-V$ scanning tends to reduce the extent of hysteresis.

The above results specifically concern $CH_3NH_3PbI_3$ and may not be commonly observed for other organo-lead halide perovskites. It is generally assessed that ferroelectricity of $CH_3NH_3PbI_3$ is weak when estimated for the bulk crystal. However, ferroelectric polarization can be enhanced in the thin film form being exposed to a large electric field. Polarization of the $CH_3NH_3PbI_3$ film is thought to be very sensitive to external bias especially for continuous flat structured (planar) bulk layers. Such polarization must be intensified when the bias voltage exceeds a threshold value that can generate a strong external field (E_{ext}) to develop an ordered array of dipoles. In the results of Figures 3 and 4, we see large hysteresis occurring by the threshold bias voltage at around −0.5 V. We found that this threshold voltage in the reverse bias condition is also related to enhancement of the photoconductivity in $CH_3NH_3PbI_3$, possibly as a result of dipole orientation. This enhanced photoconductivity exhibits generation of large photocurrent density (100−300 mA cm^{-2}) as a large-gain photodiode current. These giant photocurrents are reversibly switched off to zero current in the dark, indicating that the current enhancement is caused by a large increase in conductivity (reduced resistance) of the perovskite layer by photoexcitation in combination with dipole polarization. Figure S4 (SI) exhibits the photocurrent density profiles for forward and reverse bias conditions, measured for *meso*-TiO_2, *meso*-Al_2O_3, planar, and HTM-free planar structures of perovskite solar cells. Here, the HTM-free and symmetrical structures gave symmetrical switching behavior in photocurrent generation, although the leakage dark current was large because of a poor rectification property.

In conclusion, our observation of the effect of external bias poling on different structures demonstrates that the ferroelectric polarization in the perovskite is one of the main physical mechanisms that causes the $J-V$ hysteresis. A greater magnitude of hysteresis in the case of a planar heterojunction and Al_2O_3 scaffolds in comparison to mesoporous TiO_2 structures indicates the significance of the bulk property of perovskites rich in ferroelectric domains as an origin of hysteresis. The strong influence of prebiasing of the cell on the $J-V$ characteristics was clarified. Our discovery suggests that ferroelectric polarization of perovskite layers that eventually occurred inside of the cell structure can significantly alter the cell performance and hysteresis.

■ ASSOCIATED CONTENT

Supporting Information

Experimental methods, figures, and tables, including SEM section views for perovskite solar cells, all of the photovoltaic parameters from $J-V$ measurements, and photovoltaic characteristics. This material is available free of charge via the Internet at http://pubs.acs.org.

dx.doi.org/10.1021/jz502429u | J. Phys. Chem. Lett. 2015, 6, 164−169

AUTHOR INFORMATION

Corresponding Author

*E-mail: miyasaka@toin.ac.jp. Tel: +81-45-974-5055.

Notes

The authors declare no competing financial interest.

ACKNOWLEDGMENTS

This research is supported in part by the Japan Science and Technology Agency (JST) Advanced Low Carbon Technology R&D program (ALCA). The authors thank Dr. Ajay K. Jena for his important discussion on the origin of hysteresis. H.W.C. thanks E. Sakanoshita for her device fabrication and measurements.

REFERENCES

(1) Kojima, A.; Teshima, K.; Shirai, Y.; Miyasaka, T. Organometal halide perovskites as visible-light sensitizers for photovoltaic cells. *J. Am. Chem. Soc.* **2009**, *131*, 6050−6051.

(2) Kim, H.; Lee, C.; Im, J.; Lee, K.; Moehl, T.; Marchioro, A.; Moon, S.; Humphry-Baker, R.; Yum, J.; Moser, J. E.; Grätzel, M.; Park, N. Lead iodide perovskite sensitized all-solid-state submicron thin film mesoscopic solar cell with efficiency exceeding 9%. *Sci. Rep.* **2012**, *2*, 591.

(3) Lee, M. M.; Teuscher, J.; Miyasaka, T.; Murakami, T. N.; Snaith, H. J. Efficient hybrid solar cells based on meso-superstructured organometal halide perovskites. *Science* **2012**, *338* (6107), 643−647.

(4) Liu, M.; Johnston, M.; Snaith, H. Efficient planar heterojunction perovskite solar cells by vapour deposition. *Nature* **2013**, *501*, 395−398.

(5) Guichuan, X.; Nripan, M.; Swee Sien, L.; Natalia, Y.; Xinfeng, L.; Dharani, S.; Michael, G.; Subodh, M.; Tze Chien, S. Low-temperature solution-processed wavelength-tunable perovskites for lasing. *Nat. Mater.* **2014**, *13*, 476−480.

(6) Jeon, N. J.; Noh, J. H.; Kim, Y. C.; Yang, W. S.; Ryu, S.; Seok, S. Il. Solvent engineering for high-performance inorganic−organic hybrid perovskite solar cells. *Nat. Mater.* **2014**, *13*, 897−903.

(7) Zhou, H.; Chen, Q.; Li, G.; Luo, S.; Song, T. B.; Duan, H. S.; Hong, Z.; You, J.; Liu, Y.; Yang, Y. Interface engineering of highly efficient perovskite solar cells. *Science* **2014**, *345*, 542−546.

(8) Mei, A.; Li, X.; Liu, L.; Ku, Z.; Liu, T.; Rong, Y.; Xu, M.; Hu, M.; Chen, J.; Yang, Y.; et al. A hole-conductor-free, fully printable mesoscopic perovskite solar cell with high stability. *Science* **2014**, *345*, 295−298.

(9) Burschka, J.; Pellet, N.; Moon, S. J.; Humphry-Baker, R.; Gao, P.; Nazeeruddin, M. K.; Grätzel, M. Sequential deposition as a route to high-performance perovskite-sensitized solar cells. *Nature* **2013**, *499*, 316−319.

(10) Xiao, Z.; Bi, C.; Shao, Y.; Dong, Q.; Wang, Q.; Yuan, Y.; Wang, C.; Yongli Gao, Y.; Huang, J. Efficient, high yield perovskite photovoltaic devices grown by interdiffusion of solution-processed precursor stacking layers. *Energy Environ. Sci.* **2014**, *7*, 2619−2623.

(11) Frost, J. M.; Butler, K. T.; Walsh, A. Molecular ferroelectric contributions to anomalous hysteresis in hybrid perovskite solar cells. *Apl. Mater.* **2014**, *2*, 081506.

(12) Wei, J.; Zhao, Y.; Li, H.; Li, G.; Pan, J.; Xu, D.; Zhao, Q.; Yu, D. Hysteresis analysis based on the ferroelectric effect in hybrid perovskite solar cells. *J. Phys. Chem. Lett.* **2014**, *5*, 3937−3945.

(13) Kutes, Y.; Ye, L.; Zhou, Y.; Pang, S.; Huey, B. D.; Padture, N. P. Direct observation of ferroelectric domains in solution-processed $CH_3NH_3PbI_3$ Perovskite Thin Films. *J. Phys. Chem. Lett.* **2014**, *5*, 3335−3339.

(14) Gottesman, R.; Haltzi, E.; Gouda, L.; Tirosh, S.; Bouhadana, Y.; Zaban, A.; Mosconi, E.; De Angelis, F. Extremely slow photoconductivity response of $CH_3NH_3PbI_3$ perovskites suggesting structural changes under working conditions. *J. Phys. Chem. Lett.* **2014**, *5*, 2662−2669.

(15) Sanchez, R. S.; Gonzalez-Pedro, V.; Lee, J.-W.; Park, N.-G.; Kang, Y. S.; Mora-Sero, I.; Bisquert, J. Slow dynamic processes in lead halide perovskite solar cells. Characteristic times and hysteresis. *J. Phys. Chem. Lett.* **2014**, *5*, 2357−2363.

(16) Snaith, H. J.; Abate, A.; Ball, J. M.; Eperon, G. E.; Leijtens, T.; Noel, N. K.; Stranks, S. D.; Wang, J. T. W.; Wojciechowski, K.; Zhang, W. Anomalous hysteresis in perovskite solar cells. *J. Phys. Chem. Lett.* **2014**, *5*, 1511−1515.

(17) Unger, E. L.; Hoke, E. T.; Bailie, C. D.; Nguyen, W. H.; Bowring, A. R.; Heumuller, T.; Christoforo, M. G.; McGehee, M. D. Hysteresis and transient behavior in current-voltage measurements of hybrid-perovskite absorber solar cells. *Energy Environ. Sci.* **2014**, *7*, 3690−3698.

(18) Hui-Seon, K.; Ivan, M. S.; Victoria, G. P.; Francisco, F. S.; Emilio, J. J. P.; Nam Gyu, P.; Juan, B. Mechanism of carrier accumulation in perovskite thin-absorber solar cells. *Nature Commun.* **2013**, *4*, 2242.

(19) Juarez-Perez, E. J.; Sanchez, R. S.; Badia, L.; Garcia-Belmonte, G.; Kang, Y. S.; Mora-Sero, I.; Bisquert, J. Photoinduced giant dielectric constant in lead halide perovskite solar cells. *J. Phys. Chem. Lett.* **2014**, *5*, 2390−2394.

(20) Frost, J. M.; Butler, K. T.; Brivio, F.; Hendon, C. H.; van Schilfgaarde, M.; Walsh, A. Atomistic origins of high-performance in hybrid halide perovskite solar Cells. *Nano Lett.* **2014**, *14*, 2584−2590.

(21) Roiati, V.; Mosconi, E.; Listorti, A.; Colella, S.; Gigli, G.; De Angelis, F. Stark effect in perovskite/TiO_2 solar cells: Evidence of local interfacial order. *Nano Lett.* **2014**, *14*, 2168−2174.

(22) Stoumpos, C. C.; Malliakas, C. D.; Kanatzidis, M. G. Semiconducting tin and lead iodide perovskites with organic cations: Phase transitions, high mobilities, and near-infrared photoluminescent properties. *Inorg. Chem.* **2013**, *52*, 9019−9038.